Macromolecules

Article

Cite This: Macromolecules 2017, 50, 8562-8569

pubs.acs.org/Macromolecules

Improving the Folding of Supramolecular Copolymers by Controlling the Assembly Pathway Complexity

Gijs M. ter Huurne, Lafayette N. J. de Windt, Yiliu Liu, E. W. Meijer, Ilja K. Voets,* and Anja R. A. Palmans*

Institute for Complex Molecular Systems, Laboratory of Macromolecular and Organic Chemistry, Eindhoven University of Technology, P.O. Box 513, 5600 MB Eindhoven, The Netherlands

Supporting Information

ABSTRACT: A family of amphiphilic, heterograft copolymers containing hydrophilic, hydrophobic, and supramolecular units based on Jeffamine M-1000, dodecylamine, and benzene-1,3,5-tricarboxamide (BTA) motifs, respectively, was prepared via a postfunctionalization approach. The folding of the copolymers in water into nanometer-sized particles was analyzed by a combination of dynamic and static light scattering, circular dichroism spectroscopy, and small-angle neutron scattering. The sample preparation protocol was crucial for obtaining reproducible and consistent results, showing that only full control over the structure and pathway complexity will afford the desired folded structure, a phenomenon similar to protein folding. The results revealed that relatively small changes in the polymer's graft composition strongly affected the intra- versus intermolecular assembly processes. Depending on the amount of the hydrophobic grafts based on either dodecyl or BTA groups, pronounced behavioral differences were observed for copolymers that comprise similar degrees of hydrophobic content. A high number of BTA grafts (>10%) resulted in the formation of multichain aggregates comprising around six polymer chains. In contrast, for copolymers comprising up to 10% BTA grafts the folding results in nanoparticles that adopt open, sparse conformations and comprise one to two polymer chains. Interestingly, predominantly single-chain polymeric nanoparticles were formed when the copolymer comprised only Jeffamine or Jeffamine and dodecyl grafts. In addition, replacing part of the BTA grafts by hydrophobic dodecyl grafts while keeping the hydrophobic content constant promoted single-chain folding and resulted in the formation of a compact, globular nanoparticle with a more structured interior. Thus, the intra- and intermolecular self-assembly pathways can be directed by carefully tuning the polymer's hydrophilic−hydrophobic balance in combination with the number of supramolecular grafts.

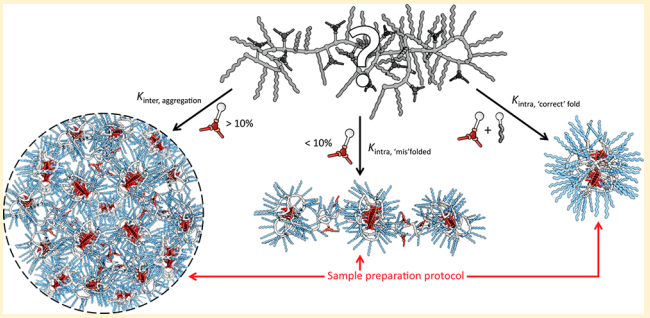

INTRODUCTION

Nature has unparalleled conformational control over its folded structures. Their ability to arrange amino acids into a precise spatial organization by way of folding allows proteins to fulfill specific functions. The well-defined binding groove in enzymes not only allows selective substrate binding but simultaneously lines up the substrate with the enzymatically active groups. The combination of these features results in extremely high catalytic activity, selectivity, and specificity. Remarkably, these complex structures result from both a delicate balance between the noncovalent interactions (for example, ionic, hydrophobic, and hydrogen-bonding interactions) that are encoded in the amino acid sequence of the protein and the pathway by which they fold.[1−3]

The relationship between the structure and function of proteins has been a major source of inspiration to the field of macromolecular science.[4] Attempts to mimic such well-defined structures have led to architectures such as dendrimers, foldamers, helical polymers, and block copolymers.[5−11] Nowadays, the use of amphiphilic heterograft copolymers to obtain macromolecular nanoparticles is gaining ground. In water, these copolymers, consisting of hydrophobic and hydrophilic grafts, collapse into a nanoparticle as a result of solvophobic interactions.[12−17] However, the precise secondary structure of proteins is not solely determined by hydrophobic and hydrophilic interactions but also relies on the formation of specific hydrogen bonds. Therefore, the folding of synthetic copolymers via hydrophobic as well as hydrogen-bonding interactions provides a fascinating route to a rudimentary protein mimic.[18,19]

A number of hydrogen-bonding supramolecular moieties have been used to fold synthetic copolymers into single-chain polymeric nanoparticles (SCPNs), such as the thymine−diaminopyridine and cyanuric acid−Hamiltonian wedge pairs as well as ureidopyrimidinones, ureas, and 2-ureido-5-deazapterinines.[18−29] In our group the ureidopyrimidinone

Received: August 16, 2017
Revised: September 27, 2017
Published: October 19, 2017

DOI: 10.1021/acs.macromol.7b01769
Macromolecules 2017, 50, 8562−8569

Scheme 1. Synthesis and Sequential Postfunctionalization of a Poly(pentafluorophenyl acrylate) Homopolymer with BTA-C_{11}-NH_2 (x), Dodecylamine (y), and Jeffamine M-1000 (z) Grafts in Various Ratios

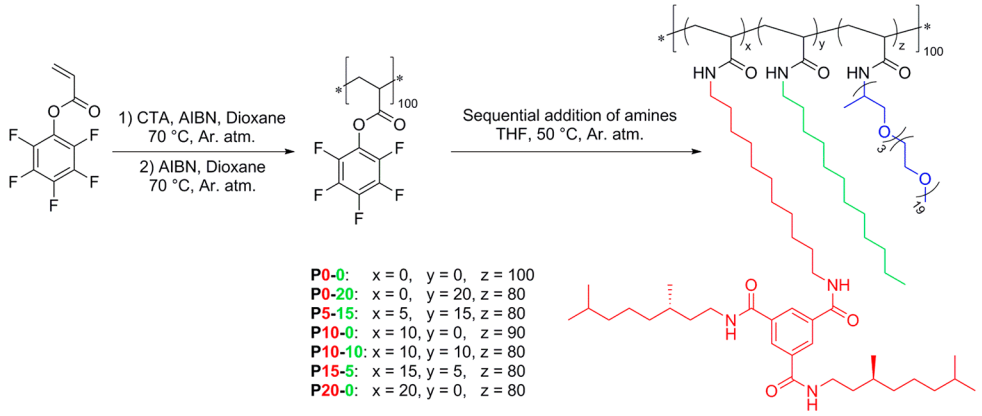

Table 1. Overview of the Polymer Composition, Number-Average Molecular Weight (M_n), Molar Mass Dispersity ($Đ_M$), and Dodecyl Equivalents of Px–y

	BTA[a] (mol %)	dodecyl[a] (mol %)	Jeffamine M-1000[a] (mol %)	$M_{n,\,SEC}$[b] (kg mol^{-1})	$Đ_M$[b]	dodecyl equiv.[c]
P0–0	0	0	100	22.8	1.16	0
P0–20	0	20	80	22.6	1.18	20
P5–15	5	15	80	22.4	1.24	30
P10–0	10	0	90	22.3	1.20	30
P10–10	10	10	80	22.7	1.23	40
P15–5	15	5	80	23.9	1.18	50
P20–0	20	0	80	23.8	1.18	60

[a]Based on the feed ratio and confirmed via ^{19}F NMR spectroscopy. [b]Determined using SEC in DMF. [c]Based on the assumption that one BTA approximately equals three dodecyl groups in terms of carbon content, so dodecyl equivalents = mol $\%_{\text{dodecyl},(y)}$ + 3·mol $\%_{\text{BTA},(x)}$.

unit and the benzene-1,3,5-tricarboxamide (BTA) moiety have been evaluated as the structuring supramolecular grafts.[30,31] The inherent ability of BTAs to self-assemble into helical supramolecular polymers—stabilized by 3-fold hydrogen bonding—make them suitable to provide structure to a polymer in solution.[32,33] In prior research, a combination of analytical techniques was applied to elucidate the details of the folding of BTA-grafted copolymers. The results showed that these amphiphilic copolymers undergo intramolecular folding via BTA self-assembly into SCPNs. However, intermolecular interactions also occur, resulting in larger, ill-defined, multi-chain aggregates.[34] In case the process of folding was dominated by intramolecular interactions, the self-assembly of BTA grafts forced the polymer chains to adopt an elongated pearl-necklace-type conformation with the self-assembly of the BTA grafts occurring in multiple domains separated along the polymer backbone.[35−37] As a result of these individually folded domains and conformational constraints of the backbone, not all BTAs can participate in the formation of hydrogen-bonded structures. Such pearl-necklace-type conformations have been observed in theoretical and modeling studies focusing on the intramolecular collapse of copolymers.[38−40] The conformation of the intramolecularly folded copolymers has been shown to depend on the polymer's grafting density as well as on the backbone hydrophobicity.[41]

In this work, we perform a systematic study to elucidate the relationship between the graft composition of amphiphilic graft copolymers and their intramolecular folding behavior in aqueous solution with the aim to encode a strong propensity for SCPN formation into the molecular structure. Hereto, a set of copolymers was synthesized with varying incorporation of hydrophobic, hydrophilic, and supramolecular grafts. A combination of dynamic and static light scattering (DLS and SLS), circular dichroism (CD) spectroscopy, and small-angle neutron scattering (SANS) was used to study the interplay between the hydrophobic and hydrogen-bonding interactions on inter- and intramolecular self-assembly pathways. The results show that this interplay not only discriminates between the intra- and intermolecular assembly of the copolymers but also significantly influences the conformation and structure of the folded systems. In fact, by optimizing of the sample preparation protocol and the composition of the copolymer, we obtain compact, globular nanoparticles with a highly structured interior.

RESULTS

Synthesis and Characterization of Amphiphilic Co-polymers. A set of copolymers was synthesized using a postfunctionalization approach.[42−46] This approach has the advantage that a single polymer backbone can be used for the entire polymer family, fixing the average degree of polymerization (DP) and molar mass dispersity ($Đ_M$) of the backbone while allowing subtle changes in the graft composition. Hereto, pentafluorophenyl acrylate was polymerized using reversible addition−fragmentation chain-transfer (RAFT) polymerization. After removal of the RAFT end group, the poly(pentafluorophenyl acrylate) homopolymer (M_n = 12.8 kDa, $Đ_M$ = 1.23, DP ≈ 100) was grafted with amine-functionalized groups in a sequential fashion (Scheme 1). First, the structuring BTA-C_{11}-NH_2 grafts were introduced, followed by the hydrophobic n-dodecylamine. The polymer synthesis was completed by introduction of the hydrophilic Jeffamine M-

DOI: 10.1021/acs.macromol.7b01769
Macromolecules 2017, 50, 8562−8569

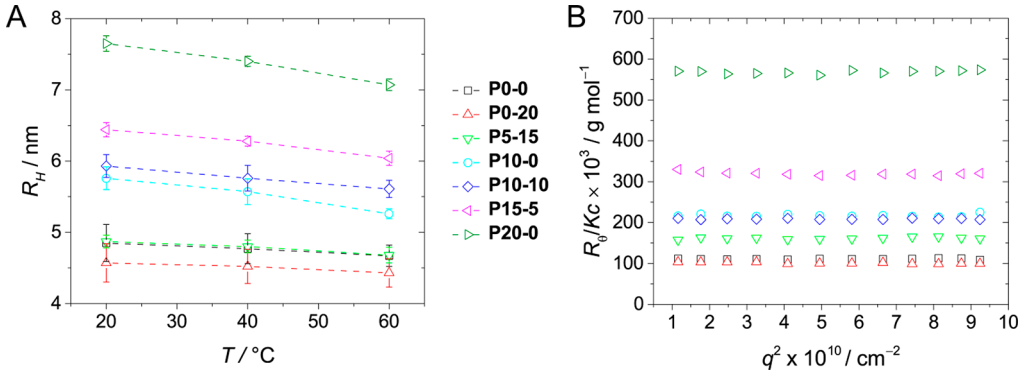

Figure 1. (A) Hydrodynamic radii (R_H) of the copolymers as a function of temperature, determined by DLS ($c_{polymer}$ = 1 mg mL^{-1}). (B) Approximate weight-average molecular weight of the nanoparticles formed by the copolymers in solution, determined via SLS ($c_{polymer}$ = 1 mg mL^{-1}, T = 20 °C, dn/dc = 0.135 mL g^{-1}).[47]

Table 2. Overview of the Effect of Polymer Composition on the Hydrodynamic Radii (R_H), the Concentration-Corrected Absolute Scattering Intensity ($R_\theta c^{-1}$), and Molar Circular Dichroism ($\Delta\varepsilon$)

	$R_{H,20\,°C}$ [a] (nm)	$R_{H,40\,°C}$ [a] (nm)	$R_{H,60\,°C}$ [a] (nm)	$R_\theta c^{-1}$ [b] (10^2 g^{-1} cm^2)	normalized $R_\theta c^{-1}$ [c]	$\Delta\varepsilon$ [d] (M^{-1} cm^{-1})
P0−0	4.9	4.8	4.6	1.47	1.0	
P0−20	4.6	4.5	4.4	1.33	0.9	
P5−15	4.9	4.8	4.7	2.13	1.4	−23
P10−0	5.8	5.6	5.3	2.87	2.0	−18
P10−10	5.9	5.8	5.6	2.76	1.9	−31
P15−5	6.4	6.3	6.0	4.22	2.9	−33
P20−0	7.7	7.4	7.1	7.50	5.1	−35

[a]Determined using DLS at the specified temperature ($c_{polymer}$ = 1 mg mL^{-1}). [b]Determined using SLS (T = 20 °C, $c_{polymer}$ = 1 mg mL^{-1}). [c]Normalized $R_\theta c^{-1} = R_\theta c^{-1}/R_\theta c^{-1}_{\mathbf{P0-0}}$. [d]Determined using CD spectroscopy (λ = 230 nm, c_{BTA} = 50 μM, T = 20 °C).

1000 groups. The conversion of each sequential postfunctionalization step was monitored using ^{19}F NMR spectroscopy by comparing the signals corresponding to the released pentafluorophenol to those of the precursor polymer. The polymers were purified via a consecutive dialysis against THF and methanol, followed by precipitation in cold *n*-pentane (see Supporting Information section 3). The final poly(acrylamide) copolymers with a DP of around 100 showed values for M_n varying between 22.3 and 23.9 kg mol^{-1} and $Đ_M$ ranging from 1.1 to 1.2 (measured by SEC in DMF). In all cases, the different grafts were randomly attached to the backbone. By tuning the incorporation ratios of the different grafts, the polymer set comprises copolymers that show a gradual change in hydrophobicity. In the nomenclature of the copolymers **P*x*−*y***, *x* is the average number of BTA units and *y* is the average number of dodecyl units attached. Assuming that the hydrophobicity of one BTA group ($C_{40}H_{70}N_3O_3$) is approximately equal to three dodecyl groups ($C_{12}H_{25}$)—based on the number of carbons of both grafts—the trend in hydrophobic content of the copolymers can be represented in terms of dodecyl equivalents, which ranges from 0 (for **P0−0**) to 60 (for **P20−0**) (Table 1).

Development of a Standard Sample Preparation Protocol. The preparation procedure of the aqueous solutions of the amphiphilic copolymers proved to be crucial to obtain reliable and reproducible data. Therefore, we started with the development of a standardized protocol affording solutions that show identical results when measured with DLS and CD spectroscopy. Several sample preparation methods were investigated, showing that not only the steps taken are important but also that their sequence plays a delicate role (see Supporting Information section 4). Ultimately, the preferred sample preparation procedure started with drying the hygroscopic copolymers using a vacuum oven at 45 °C in the presence of P_2O_5. The desired amount of dry polymer was subsequently dissolved in the appropriate amount of deionized water, sonicated (45 min), and heated (45 min at 90 °C). The samples were cooled to room temperature and allowed to equilibrate overnight before performing any further measurements.

Effect of the Polymer Design on the Polymer Solubility. The behavior of the copolymers in solution was first studied using light scattering techniques. Dynamic light scattering (DLS) was used to determine the hydrodynamic radius (R_H) based on the diffusion coefficient of the polymeric nanoparticles in solution (see Supporting Information section 5). DLS measurements show that all copolymers in solution are present as nanoparticles with hydrodynamic radii smaller than 8 nm (Figure 1A). Interestingly, the size of the nanoparticles in solution appears to be correlated to the hydrophobic content of the copolymers. The polymer with the highest hydrophobic content (**P20−0**) forms the largest nanoparticles in solution (R_H = 7.7 nm), whereas the copolymers with relative low hydrophobic contents (**P0−0**, **P0−20**, and **P5−15**) form particles with R_H below 5 nm. Furthermore, all nanoparticles appear to become slightly smaller at elevated temperatures, which is attributed to LCST-like behavior of the poly(ethylene glycol) grafts.

The R_H as determined via DLS can be influenced by interparticle interactions. Therefore, static light scattering (SLS) measurements were performed to determine the relative weight-average molecular weight of the copolymers in solution. Because of the small size of the particles in solution, the intensity of the scattered light was independent of the

DOI: 10.1021/acs.macromol.7b01769
Macromolecules 2017, 50, 8562−8569

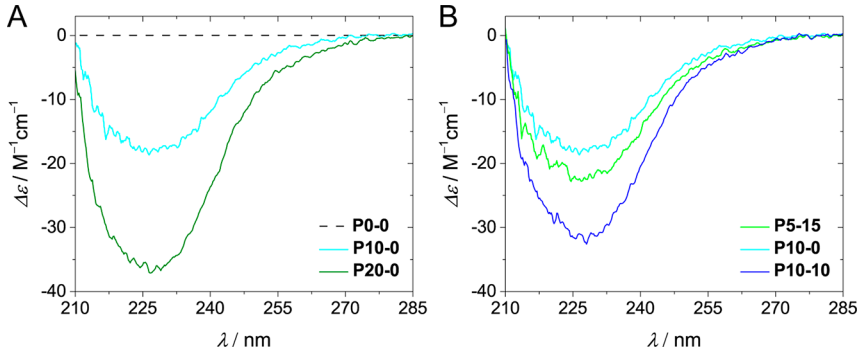

Figure 2. (A) Comparison of the CD spectra obtained for **P10−0** and **P20−0** (c_{BTA} = 50 μM, T = 20 °C). (B) Comparison of the CD spectra obtained for **P5−15**, **P10−0**, and **P20−0** (c_{BTA} = 50 μM, T = 20 °C).

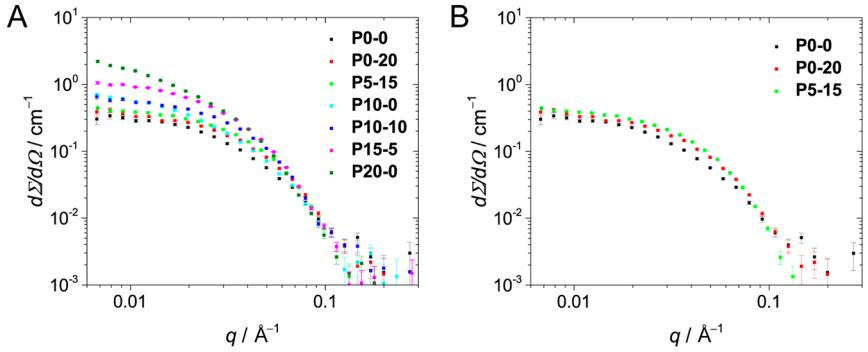

Figure 3. (A) Comparison of all the scattering curves obtained for the copolymers via SANS (T = 25 °C, $c_{polymer}$ = 1 mg mL^{-1}). (B) Scattering curves for **P0−0**, **P0−20**, and **P5−15** (T = 25 °C, $c_{polymer}$ = 1 mg mL^{-1}).

scattering angle. This angle independence in combination with an identical concentration of all samples (1 mg mL^{-1}) resulted in an absolute scattering intensity (R_θ) that only depends on the differential refractive index (dn/dc) of the polymer and the weight-average molecular weight (M_w) of the particles in solution (see Supporting Information section 5). Since all copolymers consist for the most part out of a poly(ethylene glycol) analogue (Jeffamine M-1000), we used the dn/dc reported for poly(ethylene glycol) for the calculation of the M_w.[47] The differences in the dn/dc for the different copolymers are assumed to be negligible. As a result, the absolute scattering intensities can be directly related to the M_w of the nanoparticles and thus to the aggregation number (N_{agg}) of the copolymers. Based on the relative intensities (and taking into account the determined values of R_H), **P0−0** and **P0−20** are expected to be present as individual chains in solution (Figure 1B and Table 2). The absolute scattering intensities for **P10−0** and **P10−10** are approximately twice as high, suggesting that the nanoparticles contain on average two chains. The scattering intensity of copolymer **P5−15** is in between those of the previous two cases, suggesting that it is close to being present as individual chains in solution. The polymer with the highest hydrophobic content (**P20−0**) forms the largest aggregates in solution with an estimated N_{agg} of six. Both DLS and SLS suggest that the behavior of the copolymers in solution is strongly related to their graft composition. A higher hydrophobic content leads to a larger tendency for the copolymers to cluster into multichain polymeric nanoparticles.

Effect of Copolymer Composition on the Folding Behavior. The chiral BTA grafts can be used to fold the polymer backbone into a nanoparticle via the formation of helical, hydrogen-bond-based assemblies. The presence and formation of such structured domains within the nanoparticles can be monitored using circular dichroism (CD) spectroscopy. A negative CD effect is indicative for the formation of left-handed helical BTA assemblies. In addition, the shape of the CD effect provides information on the conformation of the hydrogen-bonded amides of the BTAs in the self-assembled state, whereas the magnitude of the signal is proportional to the fraction of BTA that is helically assembled.[48,49] In fact, values for the molar circular dichroism ($\Delta\varepsilon$) at 225 nm of ±40 M^{-1} cm^{-1} indicate that all BTAs reside in a helically assembled state.[50]

For all of the BTA-containing copolymers, a negative CD effect was observed with an identical shape (see Supporting Information section 6). This similarity indicates that all of these copolymers contain structured left-handed self-assembled domains in which the amides of the BTAs adopt the same conformation. The comparison of **P10−0** and **P20−0** reveals that the value of $\Delta\varepsilon$ is more negative for a higher BTA content ($\Delta\varepsilon$ = −18 and −35 M^{-1} cm^{-1}, respectively, Figure 2A).[33] However, this trend does not hold for the entire polymer set. For example, **P5−15** shows a more intense CD effect than **P10−0** while containing only half the number of BTA grafts (Figure 2B, $\Delta\varepsilon$ = −23 and −18 M^{-1} cm^{-1}, respectively). When comparing **P10−10** and **P10−0**, the former, which contains additional dodecyl moieties, shows a CD effect that is twice as strong ($\Delta\varepsilon$ = −31 M^{-1} cm^{-1} for **P10−10**). The comparisons indicate that the graft composition of the polymer plays a key role in the degree of aggregation of the BTA pendants, which affects the folding of the polymer. The self-assembly of the BTA grafts can, for example, be significantly improved via the inclusion of additional hydrophobic grafts.

DOI: 10.1021/acs.macromol.7b01769
Macromolecules 2017, 50, 8562−8569

Table 3. Overview of the Effect of Polymer Composition on the Radius of Gyration (R_G), Particle Shape Factor (ρ), Absolute Scattering Intensity at q = 0 (I_0), Weight-Average Molecular Weight (M_w), and the Aggregation Number (N_{agg})

	R_G[a] (nm)	ρ[b]	I_0[a] (cm^{-1})	normalized I_0	$M_{w,SANS}$ (kDa)	$M_{w,calc}$[c] (kDa)	N_{agg}[d]
P0−0	5.6	1.14	0.35	1.0	65.3	127.4	0.51
P0−20	5.1	1.12	0.37	1.1	64.0	109.4	0.58
P5−15	5.1	0.86	0.43	1.2	83.1	117.9	0.70
P10−0	7.8	1.60	0.61	1.8	124.5	127.2	0.98
P10−10	5.3	0.91	0.72	2.1	191.1	119.8	1.60
P15−5	6.8	1.06	1.09	3.1	189.0	117.7	1.60
P20−0			2.20	6.4	441.6	120.5	3.66

[a]Determined using the Guinier analysis ($c_{polymer}$ = 1 mg mL^{-1}, T = 25 °C). [b]$\rho = R_G/R_H$. [c]$M_{w,calc(Px-y)} = [(M_{BTA} \times \text{mol \%}_{BTA}) + (M_{Dodecyl} \times \text{mol \%}_{dodecyl}) + (M_{Jeffamine\ M\text{-}1000} \times \text{mol \%}_{Jeffamine\ M\text{-}1000}) + M_{end\ groups}] \times Đ_{M\ (Px-y)}$. [d]$N_{agg} = M_{w,SANS}/M_{w,calc}$.

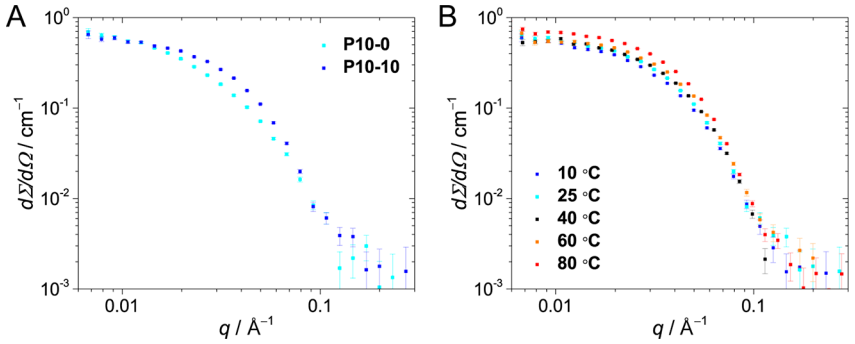

Figure 4. (A) Scattering curves for **P10−0** and **P10−0** in water ($c_{polymer}$ = 1 mg mL^{-1}, T = 25 °C). (B) Scattering curves for **P10−10** at various temperatures ($c_{polymer}$ = 1 mg mL^{-1}).

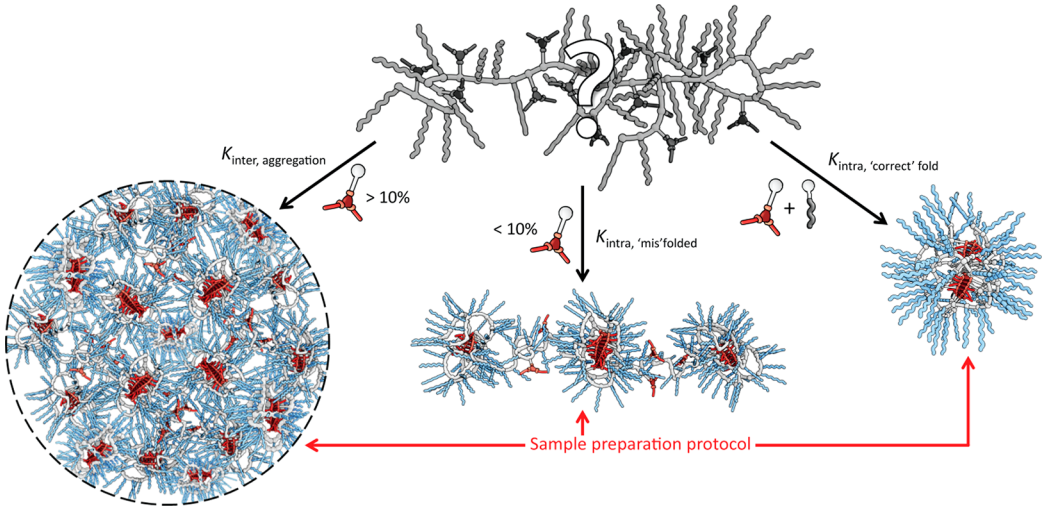

Figure 5. Schematic representation of the effect of the polymer's graft composition on the different inter- and intramolecular self-assembly pathways.

Effect of Copolymer Composition on the Polymer Conformation. Small-angle neutron scattering (SANS) experiments were performed to get insight into the relationship between the polymer's composition and its conformation in solution. The scattering profiles obtained for the different copolymers were all featureless curves leveling off at low q values, typical for small polymeric nanoparticles in solution (Figure 3A). The intensity of these plateaus at low q values was used to estimate the weight-average molecular weight of the nanoparticles in solution (Table 3; see Supporting Information section 7 for more information). Since this analysis is highly dependent on small differences in the density of the polymer samples, the calculated weights deviate from the values obtained via SLS. However, an agreement is found between the two different scattering techniques when looking at the trends.

The SANS results indicate that the aggregation number of the copolymers is related to the hydrophobic content of the copolymers, corroborating the SLS results. Whereas **P0−0**, **P0−20**, and **P5−15** are present as individual chains in solution, the copolymers with a higher BTA content form dimers (**P10−0** and **P10−10**) or larger aggregates (**P15−5** and **P20−0**). The scattering curves of the copolymers present as unimers (**P0−0**, **P0−20**, and **P5−15**) show a steeper decay in the scattering profiles for **P0−20** and **P5−15** than for **P0−0**, which indicates that **P0−20** and **P5−15** adopt a more compact conformation than **P0−0** (Figure 3B). This difference is attributed to a more pronounced hydrophobic collapse resulting from the higher

DOI: 10.1021/acs.macromol.7b01769
Macromolecules 2017, 50, 8562−8569

hydrophobic content of **P0−20** and **P5−15**. Furthermore, the particle shape factor (ρ) obtained for **P5−15** indicates that this BTA-containing polymer forms compact globular nanoparticles as the ρ value (0.86) approaches that for a perfect sphere (ρ = 0.775).

The longer plateau at low q values followed by the steeper decay of **P10−10**'s scattering profile indicates that the presence of the additional dodecyl groups results in significantly smaller and more compact nanoparticles (Figure 4A). This difference is supported by the obtained particle shape factors, which shows that **P10−10** is present as a globular particle compared to **P10−0**, which is more asymmetrically shaped.

Temperature-dependent SANS experiments were performed to study the effect of temperature on **P10−10**'s conformation. Upon increasing the temperature, the polymer appears to adopt a slightly more compact and globular conformation (Figure 4B). This change can be attributed to both the LCST-like behavior of the hydrophilic grafts and the BTAs being assembled to a lesser extent.[35,36] When the interior is less structured by hydrogen bonds, the polymer has the conformational freedom needed to adopt a more globular structure.

DISCUSSION

By comparing subsets of this novel family of BTA-based amphiphilic graft copolymers, the influence of specific grafts on the folding behavior of the copolymer in water can be elucidated. The proposed relationship between the copolymer's graft composition and the concomitant self-assembly pathways are illustrated in Figure 5.

The effect of the structuring BTA moiety on the propensity of the copolymers to aggregate can be deduced by comparing **P0−0**, **P10−0**, and **P20−0**. DLS measurements show that the particle size increases as a function of the BTA incorporation. SLS experiments indicate that the increase in particle size is associated with an increase in the polymer's aggregation number. While **P0−0** is present as individual polymer chains in solution, **P10−0** and **P20−0** form dimeric and oligomeric nanoparticles, respectively. Apparently, the tendency of BTA to form hydrogen-bonded structures in combination with its hydrophobic nature induces the intermolecular self-assembly of the copolymers into aggregates. The increase in hydrogen-bond formation between BTAs for **P20−0** is reflected by a larger value of $\Delta\varepsilon$, suggesting that the increase in particle size is driven by hydrophobic and hydrogen-bonding interactions.

The effect of the dodecyl grafts as an additional hydrophobic moiety on the folding behavior of the copolymers is highlighted by comparing **P10−0** with **P10−10**. Light scattering shows that the two copolymers are similar in terms of size (R_h = 5.8−5.9 nm) and aggregation number ($N_{agg} \approx 2$), which suggests that the incorporation of 10 mol % of additional dodecyl grafts does not enhance polymer aggregation. Interestingly, although the two copolymers contain a similar number of BTAs per chain, the $\Delta\varepsilon$ of **P10−10** is twice as large as that of **P10−0**. This difference shows that the extent of BTA self-assembly is significantly larger for the polymer containing the additional hydrophobic grafts. Besides being more structured, the SANS experiments indicate that the particles formed by **P10−10** are more globular and compact than **P10−0**, highlighting the importance of the copolymer's grafting density as well as the overall hydrophobicity.

The beneficial effect of incorporating both BTA and dodecyl grafts is culminated in **P5−15**. CD spectroscopy shows that **P5−15** has a $\Delta\varepsilon$ of −23 M^{-1} cm^{-1}, which is stronger than that observed for **P10−0** ($\Delta\varepsilon$ = −18 M^{-1} cm^{-1}) despite the fact that the latter comprises twice the amount of BTAs. In addition, the lower BTA content reduces the propensity to aggregate, as both the size and aggregation number of the copolymer in solution indicate single-chain folding. The combination of the different techniques shows that at 5 and 15 mol % of BTA and dodecyl grafts, respectively, the polymer folds intramolecularly in an efficient way into a compact, globular particle.

Finally, in comparison to the previously studied methacrylate-based amphiphilic copolymers,[33,35,36] **P10−0** and **P10−10** are on average both present as dimers. This discrepancy is tentatively attributed to the use of a different polymer backbone as well as a different hydrophilic graft in comparison to those applied in our previous studies, in which a poly(methacrylate) backbone and oligo(ethylene glycol) grafts were used. The ability of the poly(acrylamide) backbone to form hydrogen bonds and the hydrophobic propylene oxide units of the Jeffamine M-1000 grafts in close vicinity to the polymer backbone seemingly alters the hydrophilic−hydrophobic balance of the copolymers such that dimerization is more favored.

CONCLUSIONS

A systematic study was performed to elucidate the relation between the molecular design of foldable copolymers and their folding behavior in solution. By means of a combination of DLS, SLS, CD spectroscopy, and SANS, we show that relatively small changes in molecular design impart a significant effect on the behavior of the polymer in solution. By tuning the composition of the amphiphilic heterograft copolymer, the balance between hydrophobicity and hydrophilicity can be altered, which permits to control both the intra- and intermolecular self-assembly pathways of the copolymers. The scattering experiments suggest that the aggregation of the copolymers in solution is strongly related to their BTA content. Lowering the incorporation of the supramolecular graft promotes the intramolecular self-assembly of the polymer, presumably by improving the hydrophilic−hydrophobic balance. In contrast, incorporation of 20 mol % of a smaller hydrophobic group in the form of a dodecyl group does not induce aggregation of the copolymers. Intriguingly, the inclusion of additional dodecyl chains to BTA-comprising copolymers drastically enhances the folding of the copolymer as revealed by CD spectroscopy. SANS experiments show that such copolymers are not only better structured but also form more compact and smaller globular structures. This research will contribute to further understanding the relationship between a polymer's design and its behavior in solution. We anticipate that this increased understanding will improve our ability to design SCPN-based systems that show, for example, enhanced catalytic efficiencies and stabilities. Such insights are essential to prepare nanoparticles capable of fulfilling efficient and specific functions.

ASSOCIATED CONTENT

Supporting Information

The Supporting Information is available free of charge on the ACS Publications website at DOI: 10.1021/acs.macromol.7b01769.

Detailed synthetic and experimental procedures, ^{1}H NMR spectroscopy, dynamic light scattering, static light

DOI: 10.1021/acs.macromol.7b01769
Macromolecules 2017, 50, 8562−8569

scattering, circular dichroism spectroscopy, and small-angle neutron scattering (PDF)

AUTHOR INFORMATION

Corresponding Authors

*(A.R.A.P.) E-mail a.palmans@tue.nl, tel 0031 40 247 3105.
*(I.K.V.) E-mail i.voets@tue.nl, tel 0031 40 247 5303.

ORCID

E. W. Meijer: 0000-0003-4126-7492
Anja R. A. Palmans: 0000-0002-7201-1548

Notes

The authors declare no competing financial interest.

ACKNOWLEDGMENTS

This work is financed by the Dutch Ministry of Education, Culture and Science (Gravity program 024.001.035). I.K.V. is grateful for financial support from The Netherlands Organization for Scientific research (NWO VIDI grant: 7h23.014.006, ECHO-STIP 717.013.005). The ICMS Animation Studio (Eindhoven University of Technology) is acknowledged for providing the artwork. The small-angle neutron scattering experiments were performed at the LARMOR beamline of ISIS, situated at the Rutherford Appleton Laboratory of the Science and Technology Facilities Council, on the Harwell Science and Innovation Campus in Oxfordshire, United Kingdom. We thank Dr. Robert Dalgliesh for his assistance.

REFERENCES

(1) Anfinsen, C. B. Principles That Govern the Folding of Protein Chains. *Science* **1973**, *181*, 223−230.
(2) Dobson, C. M. Protein Folding and Misfolding. *Nature* **2003**, *426*, 884−890.
(3) Sadowski, M. I.; Jones, D. T. The Sequence−structure Relationship and Protein Function Prediction. *Curr. Opin. Struct. Biol.* **2009**, *19*, 357−362.
(4) Lutz, J.-F.; Lehn, J.-M.; Meijer, E. W.; Matyjaszewski, K. From Precision Polymers to Complex Materials and Systems. *Nat. Rev. Mater.* **2016**, *1*, 16024.
(5) Tomalia, D. A.; Fréchet, J. M. J. Discovery of Dendrimers and Dendritic Polymers: A Brief Historical Perspective. *J. Polym. Sci., Part A: Polym. Chem.* **2002**, *40*, 2719−2728.
(6) Bosman, A. W.; Janssen, H. M.; Meijer, E. W. About Dendrimers: Structure, Physical Properties, and Applications. *Chem. Rev.* **1999**, *99*, 1665−1688.
(7) Hill, D. J.; Mio, M. J.; Prince, R. B.; Hughes, T. S.; Moore, J. S. A Field Guide to Foldamers. *Chem. Rev.* **2001**, *101*, 3893−4011.
(8) Yashima, E.; Ousaka, N.; Taura, D.; Shimomura, K.; Ikai, T.; Maeda, K. Supramolecular Helical Systems: Helical Assemblies of Small Molecules, Foldamers, and Polymers with Chiral Amplification and Their Functions. *Chem. Rev.* **2016**, *116*, 13752−13990.
(9) Patterson, J. P.; Robin, M. P.; Chassenieux, C.; Colombani, O.; O'Reilly, R. K. The Analysis of Solution Self-Assembled Polymeric Nanomaterials. *Chem. Soc. Rev.* **2014**, *43*, 2412−2425.
(10) O'Reilly, R. K.; Hawker, C. J.; Wooley, K. L. Cross-Linked Block Copolymer Micelles: Functional Nanostructures of Great Potential and Versatility. *Chem. Soc. Rev.* **2006**, *35*, 1068−1083.
(11) Mai, Y.; Eisenberg, A. Self-Assembly of Block Copolymers. *Chem. Soc. Rev.* **2012**, *41*, 5969−5985.
(12) Morishima, Y.; Nomura, S.; Ikeda, T.; Seki, M.; Kamachi, M. Characterization of Unimolecular Micelles of Random Copolymers of Sodium 2-(Acrylamido)-2-Methylpropanesulfonate and Methacrylamides Bearing Bulky Hydrophobic Substituents. *Macromolecules* **1995**, *28*, 2874−2881.
(13) Yusa, S. I.; Sakakibara, A.; Yamamoto, T.; Morishima, Y. Fluorescence Studies of pH-Responsive Unimolecular Micelles Formed from Amphiphilic Polysulfonates Possessing Long-Chain Alkyl Carboxyl Pendants. *Macromolecules* **2002**, *35*, 10182−10188.
(14) Chen, H.; Zhang, Q.; Li, J.; Ding, Y.; Zhang, G.; Wu, C. Formation of Mesoglobular Phase of PNIPAM-G-PEO Copolymer with a High PEO Content in Dilute Solutions. *Macromolecules* **2005**, *38*, 8045−8050.
(15) Akagi, T.; Piyapakorn, P.; Akashi, M. Formation of Unimer Nanoparticles by Controlling the Self-Association of Hydrophobically Modified Poly(amino Acid)s. *Langmuir* **2012**, *28*, 5249−5256.
(16) Terashima, T.; Sugita, T.; Fukae, K.; Sawamoto, M. Synthesis and Single-Chain Folding of Amphiphilic Random Copolymers in Water. *Macromolecules* **2014**, *47*, 589−600.
(17) Liu, R. C. W.; Pallier, A.; Brestaz, M.; Pantoustier, N.; Tribet, C. Impact of Polymer Microstructure on the Self-Assembly of Amphiphilic Polymers in Aqueous Solutions. *Macromolecules* **2007**, *40*, 4276−4286.
(18) Mavila, S.; Eivgi, O.; Berkovich, I.; Lemcoff, N. G. Intramolecular Cross-Linking Methodologies for the Synthesis of Polymer Nanoparticles. *Chem. Rev.* **2016**, *116*, 878−961.
(19) Lyon, C. K.; Prasher, A.; Hanlon, A. M.; Tuten, B. T.; Tooley, C. A.; Frank, P. G.; Berda, E. B. A Brief User's Guide to Single-Chain Nanoparticles. *Polym. Chem.* **2015**, *6*, 181−197.
(20) Deans, R.; Ilhan, F.; Rotello, V. M. Recognition-Mediated Unfolding of a Self-Assembled Polymeric Globule. *Macromolecules* **1999**, *32*, 4956−4960.
(21) Seo, M.; Beck, B. J.; Paulusse, J. M. J.; Hawker, C. J.; Kim, S. Y. Polymeric Nanoparticles via Noncovalent Cross-Linking of Linear Chains. *Macromolecules* **2008**, *41*, 6413−6418.
(22) Matsumoto, K.; Terashima, T.; Sugita, T.; Takenaka, M.; Sawamoto, M. Amphiphilic Random Copolymers with Hydrophobic/Hydrogen-Bonding Urea Pendants: Self-Folding Polymers in Aqueous and Organic Media. *Macromolecules* **2016**, *49*, 7917−7927.
(23) Wang, F.; Pu, H.; Jin, M.; Pan, H.; Chang, Z.; Wan, D.; Du, J. From Single-Chain Folding to Polymer Nanoparticles via Intramolecular Quadruple Hydrogen-Bonding Interaction. *J. Polym. Sci., Part A: Polym. Chem.* **2015**, *53*, 1832−1840.
(24) Romulus, J.; Weck, M. Single-Chain Polymer Self-Assembly Using Complementary Hydrogen Bonding Units. *Macromol. Rapid Commun.* **2013**, *34*, 1518−1523.
(25) Altintas, O.; Lejeune, E.; Gerstel, P.; Barner-Kowollik, C. Bioinspired Dual Self-Folding of Single Polymer Chains via Reversible Hydrogen Bonding. *Polym. Chem.* **2012**, *3*, 640−651.
(26) Foster, E. J.; Berda, E. B.; Meijer, E. W. Metastable Supramolecular Polymer Nanoparticles via Intramolecular Collapse of Single Polymer Chains. *J. Am. Chem. Soc.* **2009**, *131*, 6964−6966.
(27) Berda, E. B.; Foster, E. J.; Meijer, E. W. Toward Controlling Folding in Synthetic Polymers: Fabricating and Characterizing Supramolecular Single-Chain Nanoparticles. *Macromolecules* **2010**, *43*, 1430−1437.
(28) Stals, P. J. M.; Gillissen, M. A. J.; Nicolaÿ, R.; Palmans, A. R. A.; Meijer, E. W. The Balance between Intramolecular Hydrogen Bonding, Polymer Solubility and Rigidity in Single-Chain Polymeric Nanoparticles. *Polym. Chem.* **2013**, *4*, 2584−2597.
(29) ter Huurne, G. M.; Gillissen, M. A. J.; Palmans, A. R. A.; Voets, I. K.; Meijer, E. W. The Coil-to-Globule Transition of Single-Chain Polymeric Nanoparticles with a Chiral Internal Secondary Structure. *Macromolecules* **2015**, *48*, 3949−3956.
(30) Mes, T.; van der Weegen, R.; Palmans, A. R. A; Meijer, E. W. Single-Chain Polymeric Nanoparticles by Stepwise Folding. *Angew. Chem., Int. Ed.* **2011**, *50*, 5085−5089.
(31) Hosono, N.; Gillissen, M. A. J.; Li, Y.; Sheiko, S. S.; Palmans, A. R. A; Meijer, E. W. Orthogonal Self-Assembly in Folding Block Copolymers. *J. Am. Chem. Soc.* **2013**, *135*, 501−510.
(32) Cantekin, S.; de Greef, T. F. A.; Palmans, A. R. A. Benzene-1,3,5-Tricarboxamide: A Versatile Ordering Moiety for Supramolecular Chemistry. *Chem. Soc. Rev.* **2012**, *41*, 6125−6137.
(33) Terashima, T.; Mes, T.; De Greef, T. F. A.; Gillissen, M. A. J.; Besenius, P.; Palmans, A. R. A.; Meijer, E. W. Single-Chain Folding of

DOI: 10.1021/acs.macromol.7b01769
Macromolecules 2017, 50, 8562−8569

Polymers for Catalytic Systems in Water. *J. Am. Chem. Soc.* **2011**, *133*, 4742−4745.
(34) Altintas, O.; Artar, M.; ter Huurne, G. M.; Voets, I. K.; Palmans, A. R. A.; Barner-Kowollik, C.; Meijer, E. W. Design and Synthesis of Triblock Copolymers for Creating Complex Secondary Structures by Orthogonal Self-Assembly. *Macromolecules* **2015**, *48*, 8921−8932.
(35) Gillissen, M. A. J.; Terashima, T.; Meijer, E. W.; Palmans, A. R. A.; Voets, I. K. Sticky Supramolecular Grafts Stretch Single Polymer Chains. *Macromolecules* **2013**, *46*, 4120−4125.
(36) Stals, P. J. M.; Gillissen, M. A. J.; Paffen, T. F. E.; de Greef, T. F. A.; Lindner, P.; Meijer, E. W.; Palmans, A. R. A.; Voets, I. K. Folding Polymers with Pendant Hydrogen Bonding Motifs in Water: The Effect of Polymer Length and Concentration on the Shape and Size of Single-Chain Polymeric Nanoparticles. *Macromolecules* **2014**, *47*, 2947−2954.
(37) Hosono, N.; Palmans, A. R. A; Meijer, E. W. "Soldier-Sergeant-Soldier" Triblock Copolymers: Revealing the Folded Structure of Single-Chain Polymeric Nanoparticles. *Chem. Commun.* **2014**, *50*, 7990−7993.
(38) Dobrynin, A. V.; Rubinstein, M.; Obukhov, S. P. Cascade of Transitions of Polyelectrolytes in Poor Solvents. *Macromolecules* **1996**, *29*, 2974−2979.
(39) Hugouvieux, V.; Axelos, M. A. V.; Kolb, M. Amphiphilic Multiblock Copolymers: From Intramolecular Pearl Necklace to Layered Structures. *Macromolecules* **2009**, *42*, 392−400.
(40) Borisov, O. V.; Zhulina, E. B. Amphiphilic Graft Copolymer in a Selective Solvent: Intramolecular Structures and Conformational Transitions. *Macromolecules* **2005**, *38*, 2506−2514.
(41) Košovan, P.; Kuldová, J.; Limpouchová, Z.; Procházka, K.; Zhulina, E. B.; Borisov, O. V. Amphiphilic Graft Copolymers in Selective Solvents: Molecular Dynamics Simulations and Scaling Theory. *Macromolecules* **2009**, *42*, 6748−6760.
(42) Eberhardt, M.; Mruk, R.; Zentel, R.; Théato, P. Synthesis of Pentafluorophenyl(meth)acrylate Polymers: New Precursor Polymers for the Synthesis of Multifunctional Materials. *Eur. Polym. J.* **2005**, *41*, 1569−1575.
(43) Eberhardt, M.; Théato, P. RAFT Polymerization of Pentafluorophenyl Methacrylate: Preparation of Reactive Linear Diblock Copolymers. *Macromol. Rapid Commun.* **2005**, *26*, 1488−1493.
(44) Theato, P. Synthesis of Well-Defined Polymeric Activated Esters. *J. Polym. Sci., Part A: Polym. Chem.* **2008**, *46*, 6677−6687.
(45) Liu, Y.; Pauloehrl, T.; Presolski, S. I.; Albertazzi, L.; Palmans, A. R. A.; Meijer, E. W. Modular Synthetic Platform for the Construction of Functional Single-Chain Polymeric Nanoparticles: From Aqueous Catalysis to Photosensitization. *J. Am. Chem. Soc.* **2015**, *137*, 13096−13105.
(46) Blasco, E.; Sims, M. B.; Goldmann, A. S.; Sumerlin, B. S.; Barner-Kowollik, C. 50th Anniversary Perspective: Polymer Functionalization. *Macromolecules* **2017**, *50*, 5215−5252.
(47) Michielsen, S. In *Polymer Handbook*, 3rd ed.; Brandrup, J., Immergut, E. H., Grulke, E. A., Eds.; John Wiley & Sons: New York, 1999.
(48) Nakano, Y.; Hirose, T.; Stals, P. J. M.; Meijer, E. W.; Palmans, A. R. A. Conformational Analysis of Supramolecular Polymerization Processes of Disc-like Molecules. *Chem. Sci.* **2012**, *3*, 148−155.
(49) Nakano, Y.; Markvoort, A. J.; Cantekin, S.; Filot, I. A. W.; ten Eikelder, H. M. M.; Meijer, E. W.; Palmans, A. R. A. Conformational Analysis of Chiral Supramolecular Aggregates: Modeling the Subtle Difference between Hydrogen and Deuterium. *J. Am. Chem. Soc.* **2013**, *135*, 16497−16506.
(50) Stals, P. J. M.; Smulders, M. M. J.; Martín-Rapún, R.; Palmans, A. R. A.; Meijer, E. W. Asymmetrically Substituted Benzene-1,3,5-tricarboxamides: Self-Assembly and Odd−Even Effects in the Solid State and in Dilute Solution. *Chem. - Eur. J.* **2009**, *15*, 2071−2080.

DOI: 10.1021/acs.macromol.7b01769
Macromolecules 2017, 50, 8562−8569